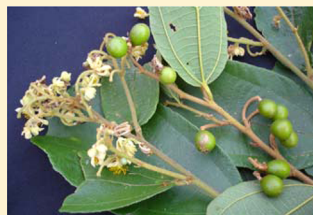


Alkaloids from *Microcos paniculata* with Cytotoxic and Nicotinic Receptor Antagonistic ActivitiesPatrick C. Still,[†] Bitna Yi,[‡] Tatiana F. González-Cestari,[‡] Li Pan,[†] Ryan E. Pavlovicz,^{†,§} Hee-Byung Chai,[†] Tran Ngoc Ninh,[‡] Chenglong Li,[†] Djaja Djendoel Soejarto,^{||,∇} Dennis B. McKay,[‡] and A. Douglas Kinghorn^{*,†}[†]Division of Medicinal Chemistry and Pharmacognosy, College of Pharmacy, The Ohio State University, Columbus, Ohio 43210, United States[‡]Division of Pharmacology, College of Pharmacy, The Ohio State University, Columbus, Ohio 43210, United States[§]Biophysics Graduate Program, The Ohio State University, Columbus, Ohio 43210, United States[‡]Institute of Ecology and Biological Resources, Vietnam Academy of Science and Technology, Hoang Quoc Viet, Cau Giay, Hanoi, Vietnam^{||}Program for Collaborative Research in the Pharmaceutical Sciences and Department of Medicinal Chemistry and Pharmacognosy, College of Pharmacy, University of Illinois at Chicago, Chicago, Illinois 60612, United States[∇]Department of Botany, Field Museum of Natural History, 1400 S. Lake Shore Drive, Chicago, Illinois 60605, United States

S Supporting Information

ABSTRACT: *Microcos paniculata* is a large shrub or small tree that grows in several countries in South and Southeast Asia. In the present study, three new piperidine alkaloids, microgrewiapienes A–C (1–3), as well as three known compounds, inclusive of microcosamine A (4), 7'-(3',4'-dihydroxyphenyl)-N-[4-methoxyphenyl]ethyl]propenamide (5), and liriodenine (6), were isolated from cytotoxic fractions of the separate chloroform-soluble extracts of the stem bark, branches, and leaves of *M. paniculata*. Compounds 1–6 and 1a (microgrewiapine A 3-acetate) showed a range of cytotoxicity values against the HT-29 human colon cancer cell line. When evaluated for their effects on human $\alpha 3\beta 4$ or $\alpha 4\beta 2$ nicotinic acetylcholine receptors (nAChRs), several of these compounds were shown to be active as nAChR antagonists. As a result of this study, microgrewiapine A (1) was found to be a selective cytotoxic agent for colon cancer cells over normal colon cells and to exhibit nicotinic receptor antagonistic activity for both the $\alpha 3\beta 4$ and $\alpha 4\beta 2$ receptor subtypes.



microgrewiapine A (1)

Microcos paniculata L. (Malvaceae) is a member of a genus having about 60 species distributed in Asia, Africa, South America, and Australia, with these plants being shrubs or small trees.¹ The dried bark, roots, fruits, and leaves of *Microcos* species have been used ethnomedicinally to treat diarrhea and fever, as general tonics, and as insecticides.^{2–4} Previous phytochemical work on the genus *Microcos* has led to reports of 2,3,6-trisubstituted piperidine alkaloids, with several substitution patterns and stereochemical configurations in the piperidine ring possible for such alkaloids.^{2–4} *M. paniculata* produces these alkaloids to defend against herbivory, with Bandara and associates having reported the insecticidal activity of a stem bark extract against the second instar larvae of the mosquito *Aedes aegypti*.³ Piperidine alkaloids of this type have also been found outside the plant kingdom, particularly corydendramines A and B from the marine hydroid *Corydendrium parasiticum* and the solenopsins from certain fire ants (*Solenopsis* spp.).^{5–8}

Identification of natural products with activities on neuronal nicotinic acetylcholine receptors (nAChRs) has substantial implications for drug discovery.^{9–11} Widely expressed through-

out the central nervous system, peripheral nervous system, and a number of peripheral organs, nAChRs are ligand-gated ion channels that mediate acetylcholine-mediated signaling, and thus contribute to a wide range of physiological processes such as pain, cognition, fast synaptic transmission, and inflammation.^{9,10,12} Associated with various diseases and disorders (e.g., depression, anxiety, autism, ADHD, schizophrenia, and cancer), nAChRs have been a focus of drug discovery efforts as an attractive therapeutic target.^{9–11,13}

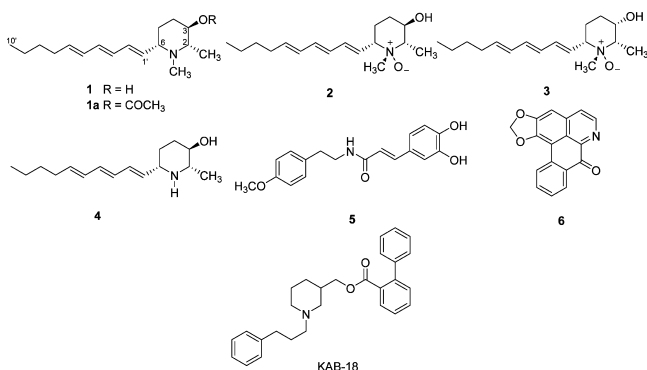
Reported herein is the purification of three new piperidine alkaloids, microgrewiapienes A–C (1–3), and three known compounds, microcosamine A (4), 7'-(3',4'-dihydroxyphenyl)-N-[4-methoxyphenyl]ethyl]propenamide (5), and liriodenine (6), from the separate stem bark, branches, and leaves of *M. paniculata*. All plant parts were collected in Vietnam as part of an ongoing investigation on the discovery of natural anticancer agents from tropical plants. Chloroform extracts were purified,

Received: October 24, 2012

Published: January 17, 2013

and their anticancer potential was evaluated by testing cytotoxic effects against the HT-29 human colon cancer cell line.¹⁴ The structures of the three new compounds were established by spectroscopic data interpretation. Esterification at the C-3 hydroxy group using the Mosher ester method allowed unambiguous assignment of the absolute configuration of compound 1. The three known compounds 4–6 were identified by spectroscopic analysis and comparison of the data obtained with literature values.^{4,15,16} Structural similarity of compounds 1–4 to the previously identified nAChR antagonist 1-(3-phenylpropyl)piperidin-3-yl)methyl [1,1'-biphenyl]-2-carboxylate (KAB-18), along with growing evidence to support the involvement of nAChRs in various aspects of cancer, provided a rationale to examine the effects of 1–6 on nAChRs.^{17–19}

As a result of this study, microgrewapipe A (1) was found to be a cytotoxic agent against HT-29 human colon cancer cells and to exhibit nicotinic receptor antagonistic activity for both the $\alpha 3\beta 4$ and $\alpha 4\beta 2$ receptor subtypes. This is the first report of cytotoxicity and nAChR modulatory activity of piperidine alkaloids from a plant in the genus *Microcos*.



RESULTS AND DISCUSSION

Microgrewapipe A (1) was obtained as colorless needle crystals, mp 127–128 °C, $[\alpha]_{\text{D}}^{15} +15.4$ (c 0.1, MeOH). A

molecular formula of $\text{C}_{17}\text{H}_{29}\text{NO}$ was determined from the molecular ion peak at m/z 264.2329 $[\text{M} + \text{H}]^+$ (calcd for $\text{C}_{17}\text{H}_{30}\text{NO}$, 264.2327) in the HRESIMS, which supported the presence of a single nitrogen atom in the molecule. The IR spectrum showed bands at 3402, 2929, and 1629 cm^{-1} , indicative of hydroxy group absorption and olefinic C–H stretching, respectively. The UV spectrum exhibited a maximum at 270 nm, suggesting conjugation in the molecule. The ^1H NMR and ^{13}C NMR spectra (600 MHz, CDCl_3 , Table 1) showed signals for six methine groups in the region δ_{H} 5.53–6.16, along with resonances at δ_{H} 2.09 (2H, dt, $J = 7.2, 6.9$ Hz, H-7'), 1.29–1.38 (4H, H-8', H-9'), and 0.89 (3H, t, $J = 7.2$ Hz, H-10'), which correlated in the ^1H - ^{13}C HSQC spectrum to six olefinic methine carbons [δ_{C} 130.1–136.7], three methylene carbons [δ_{C} 32.5 (C-7'); 31.4 (C-8'); 22.0 (C-9')], and a methyl carbon [δ_{C} 14.1 (C-10')], respectively. These NMR signals indicated the presence of a deca-trienyl group in the molecule of 1. Double-bond geometry at $\Delta^{1',2'}$ and $\Delta^{5',6'}$ was determined to be *trans* on the basis of the large coupling constants $J_{1',2'} = 14.6$ Hz and $J_{5',6'} = 14.5$ Hz. For $\Delta^{3',4'}$, the configuration could not be determined by coupling constants due to signal overlap. Differences in ^1H and ^{13}C chemical shifts between (1'E,3'E,5'E) and (1'E,3'Z,5'E) geometries, however, can be used to elucidate the $\Delta^{3',4'}$ configuration. If the conjugated triene system adopts a (1'E,3'E,5'E) geometry, the NMR chemical shifts of H-2'/H-5' and C-2'/C-5' are typically around δ_{H} 6.0 ppm and δ_{C} 130 ppm, respectively.²⁰ If the conjugated triene instead adopts a (1'E,3'Z,5'E) geometry, δ_{H} H-2'/H-5' shifts ~ 0.4 ppm downfield and δ_{C} C-2'/C-5' shifts ~ 5 ppm upfield.²⁰ The triene system of 1 shows chemical shifts of δ_{H} 6.03–6.16 (H-2', H-5') and δ_{C} 130.1–132.6 (C-2', C-5'), which support a *trans* configuration for $\Delta^{3',4'}$. The remaining ^1H and ^{13}C NMR signals were attributed to a methyl group [δ_{H} 1.26 (3H, d, $J = 6.1$ Hz, CH_3 -2); δ_{C} 16.4], two methylene groups [δ_{H} 2.03 (1H, m, H-4 α), 1.29–1.38 (1H, H-4 β), 1.49 (1H, ddd, $J = 10.1, 3.0, 3.0$ Hz, H-5 α), 1.63 (1H, m, H-5 β); δ_{C} 33.5 (C-4), 31.3 (C-5)], an oxygen-bearing methine group [δ_{H} 3.27 (1H, ddd, $J = 10.8, 8.9, 4.5$, H-3); δ_{C} 72.6 (C-3)], two nitrogen-bearing methine

Table 1. ^1H NMR and ^{13}C NMR Data for 1–3^a

no.	1		2		3	
	δ_{C}	δ_{H} (J in Hz)	δ_{C}	δ_{H} (J in Hz)	δ_{C}	δ_{H} (J in Hz)
2	66.1	1.83, dq (8.9, 6.1)	76.5	2.86, dq (10.7, 6.1)	68.6	3.05, dq (12.7, 6.5)
3	72.6	3.27, ddd (10.8, 8.9, 4.5)	67.4	3.90, ddd (11.2, 10.5, 4.8)	71.1	3.82, brs
4 α	33.5	2.03, m	33.0	1.46, m	32.1	1.57, m
4 β		1.29–1.38 ^b		2.13, m		2.01, m
5 α	31.3	1.49, ddd (10.1, 3.0, 3.0)	26.6	2.33, m	23.8	1.56, m
5 β		1.63, m		1.62, m		2.67, ddd (12.0, 4.1, 3.6)
6	67.6	2.48, ddd (11.2, 8.7, 3.0)	78.8	3.44, m	79.5	3.53, ddd (11.4, 9.4, 1.9)
1'	136.7	5.53, dt (14.6, 8.8)	127.7	5.94, dt (15.3, 8.9)	127.9	5.98, dt (15.1, 7.0)
2'-5'	130.1–132.6	6.03–6.16 ^b	128.8–135.8	6.05–6.26 ^b	129.2–136.1	5.96–6.25 ^b
6'	135.7	5.71, dd (14.5, 7.4)	137.6	5.74, dd (14.2, 7.2)	137.8	5.72, dd (15.2, 9.0)
7'	32.5	2.09, dt (7.2, 6.9)	32.9	2.09, dt (7.2, 6.9)	32.7	2.09, dt (7.0, 6.2)
8', 9'	31.4; 22.0	1.29–1.38 ^b	30.9; 21.8	1.26–1.41 ^b	31.5; 22.5	1.24–1.39 ^b
10'	14.1	0.89, t (7.2)	14.3	0.89, t (7.0)	14.1	0.89, t (7.1)
CH_3 -2	16.4	1.26, d (6.1)	10.6	1.57, d (6.0)	13.5	1.66, d (6.5)
N- CH_3	40.4	2.21, s	51.1	2.95	54.1	2.86, s

^aCompound 1 measured at 600 MHz, compounds 2 and 3 measured at 400 MHz. All compound NMR spectra obtained in CDCl_3 with TMS as internal standard; J values (Hz) are given in parentheses. Assignments supported with ^1H - ^1H COSY, HSQC, and HMBC spectra. ^bMultiplicity patterns unclear due to signal overlapping.

groups [δ_{H} 2.48 (1H, ddd, $J = 11.2, 8.7, 3.0$ Hz, H-6), 1.83 (1H, dq, $J = 8.9, 6.1$ Hz, H-2); δ_{C} 67.6 (C-6), 66.1 (C-2)], and a *N*-CH₃ group [δ_{H} 2.21 (3H, s, *N*-CH₃); δ_{C} 40.4]. The oxygen-bearing methine group at δ_{H} 3.27 (H-3) showed a ^1H – ^1H COSY correlation with the nitrogen-bearing methine group at δ_{H} 1.83 (H-2). The methylene signals δ_{H} 1.49 and 1.63, corresponding to the C-5 protons, exhibited a ^1H – ^1H COSY correlation with the nitrogen-bearing methine group at δ_{H} 2.48 (C-6). A heteronuclear ^1H – ^{13}C HMBC three-bond correlation between CH₃-2 (δ_{H} 1.26) and C-3 (δ_{C} 72.6), a four-bond correlation between the *N*-CH₃ (δ_{H} 2.21) group and CH₃-2, and a two-bond correlation between both C-5 protons and the nitrogen-bearing methine group at δ_{H} 2.48 (C-6) were observed. The chemical shift values and connectivity patterns from the ^1H – ^1H COSY and ^1H – ^{13}C HMBC spectra indicated the presence of an *N*-methyl-2-methyl-3-piperidinol ring.^{2–4} The ^1H NMR signal at δ_{H} 5.53 (1H, dt, $J = 14.6, 8.8$ Hz, H-1') was coupled to the nitrogen-bearing methine signal at δ_{H} 2.48 (C-6) with a magnitude of 8.7 Hz and also showed a ^1H – ^1H COSY correlation to the same methine proton, indicating that the deca-1*E*,3*E*,5*E*-trienyl group is attached to the *N*-methyl-2-methyl-3-piperidinol ring at C-6. The absolute configuration at the C-3 hydroxy group position was accomplished using a Mosher esterification procedure.^{21,22} Two portions of **1** (each 1.0 mg) were treated with (*S*)-(+)- α - and (*R*)-(–)- α -methoxy- α -(trifluoromethyl)phenylacetyl chloride (14 μL) in deuterated pyridine (0.5 mL) directly in separate NMR tubes at room temperature, affording the (*R*)- and (*S*)-MTPA esters, respectively.^{21,22} Observed chemical shift differences ($\Delta\delta_{\text{S-R}}$) indicated the absolute configuration at the OH-3 group of **1** to be *R* (Figure 1).

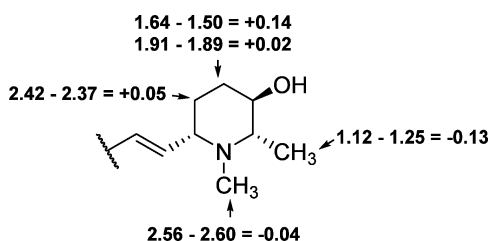


Figure 1. Chemical shift difference values, $\delta(\text{S-R})$, for protons on the esterified piperidinol ring of **1**, as established by the Mosher ester method.

With the absolute configuration at the OH-3 position determined, analysis of coupling constants and ^1H – ^1H NOESY correlations established the relative conformation of the remaining substituents of the piperidinol ring. The coupling constant between H-3 α and the signal at δ_{H} 1.83 (H-2) was 8.9 Hz, indicating the substituents were *trans* configured. Strong ^1H – ^1H NOESY correlations between H-2 and the signal at δ_{H} 2.48 (H-6) suggested that the latter proton is oriented on the β -face of the piperidinol ring with H-2 (Figure 2). Accordingly, microgrewiapine A (**1**) was assigned structurally as (2*S*,3*R*,6*S*)-6-((1*E*,3*E*,5*E*)-deca-1,3,5-trien-1-yl)-1,2-dimethylpiperidin-3-ol.

Microgrewiapine B (**2**) was obtained as a clear, amorphous solid, mp 134–136 °C, $[\alpha]_{\text{D}}^{25} +4.0$ (*c* 0.1, MeOH). A molecular formula of C₁₇H₂₉NO₂ was determined from the molecular ion peak at m/z 280.2269 [$\text{M} + \text{H}$]⁺ (calcd for C₁₇H₃₀NO₂, 280.2276) in the HRESIMS. The IR spectrum showed absorption bands at 3400, 2967, 1670, 1204, and 1000 cm^{–1}, indicative of the presence of hydroxy, olefinic C–H, C–

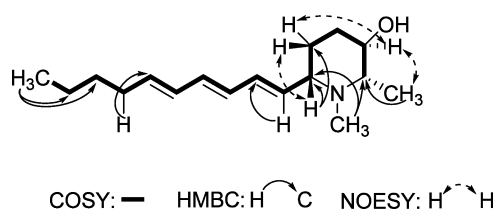


Figure 2. Key COSY, HMBC, and NOESY correlations of **1**.

N, and aliphatic amine oxide functionalities, respectively. The ^1H NMR and ^{13}C NMR spectra (400 MHz, CDCl₃, Table 1) showed that signals in the piperidine ring were shifted downfield, compared to **1**, due to the presence of an *N*-oxide moiety. Downfield shifts were pronounced in both the nitrogen-bearing methine signals at δ_{H} 2.86 (1H, dq, $J = 10.7, 6.12$ Hz, H-2) and 3.44 (1H, m, H-6) and the oxygen-bearing methine signal at δ_{H} 3.90 (1H, ddd, $J = 11.2, 10.5, 4.8$ Hz, H-3). Despite the downfield shifts of these signals, the splitting patterns were comparable to the analogous signals in compound **1** (Table 1). The coupling constant between the oxygenated methine at δ_{H} 3.90 (H-3) and the signal at δ_{H} 2.86 (H-2) was 10.7 Hz, indicating a *trans* configuration between H-3 and H-2.

Two configurations at the nitrogen atom of **2** are possible. For a 1*R* configuration, a ^1H – ^1H NOESY correlation between *N*-CH₃ and H-3 would not be expected. Indeed, no NOE correlation was observed between the signals at δ_{H} 2.95 (*N*-CH₃) and 3.90 (H-3) (Figure 3). Strong ^1H – ^1H NOESY

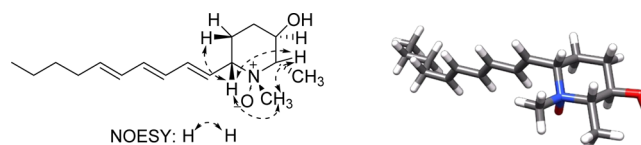


Figure 3. Key NOESY correlations and energy-minimized 3D structure of **2**.²³

correlations were seen between the *N*-methyl (δ_{H} 2.95) and H-2 (δ_{H} 2.86) signals, due to the proximity within 4 Å of these functionalities (Figure 3). In addition, ^1H – ^1H NOESY correlations were observed between the signals at δ_{H} 2.86 (H-2) and 3.44 (1H, m, H-6), indicating these protons to be located on the same face of the piperidinol ring. The ^1H NMR coupling patterns and ^1H – ^1H NOESY correlations observed for **2** were supported by in silico MP2 energy minimization studies using the 6-311G(d,p) basis set, implemented in the Gaussian 09 program.²³ Relative energies of the 1*R* and 1*S* enantiomers of **2** in the gas phase, ethanol, and water were computed, and the 1*R* enantiomer was found to be the more energetically favorable. Energy difference values between the 1*R* and 1*S* enantiomers of **2** were calculated to be 2.76, 1.08, and 0.94 kcal/mol for the gas phase, ethanol, and water, respectively. The solvent effects were calculated with a polarized continuum model that implicitly calculates the effects the solvent has on the molecule. Microgrewiapine B (**2**) was assigned structurally, therefore, as (2*S*,3*R*,6*S*)-6-((1*E*,3*E*,5*E*)-deca-1,3,5-trien-1-yl)-3-hydroxy-1,2-dimethylpiperidine 1-oxide.

Microgrewiapine C (**3**) was obtained as colorless needle crystals, mp 130–131 °C, $[\alpha]_{\text{D}}^{25} +77.8$ (*c* 0.1, MeOH). A molecular formula of C₁₇H₂₉NO₂ was determined from the molecular ion peak at m/z 280.2281 [$\text{M} + \text{H}$]⁺ (calcd for

C₁₇H₃₀NO₂, 280.2277) in the HRESIMS. The UV and IR spectra were closely comparable to those of the 3R enantiomer, **2**. The ¹H NMR signal at δ_H 3.82 (1H, brs, H-3) appeared as a broad singlet when compared to the ddd pattern as observed for **2**. The methine signal at δ_H 3.05 (1H, dq, J = 12.7, 6.5 Hz, H-2) would be expected to cause a split pattern for H-3; however no peak multiplicity was observed for this proton. The 3S configuration was supported by a strong ¹H–¹H NOESY correlation between the signals at δ_H 3.05 (1H, dq, J = 12.7, 6.5 Hz, H-2), 3.82 (1H, brs, H-3), and 3.53 (1H, ddd, J = 11.4, 9.4, 1.9 Hz, H-6), indicating that these substituents have the same orientation. In addition, a strong ¹H–¹H NOESY correlation between δ_H 2.86 (3H, s, N-CH₃) and 3.82 (1H, brs, H-3) was observed, confirming the opposite configuration from that of **2**, for which this correlation was absent. Microgrewiapipe C (**3**) was therefore assigned as (2S,3S,6S)-6-((1E,3E,5E)-deca-1,3,5-trien-1-yl)-3-hydroxy-1,2-dimethylpiperidine 1-oxide.

As part of an ongoing investigation on the discovery of natural anticancer agents from tropical plants, compounds **1–6** were evaluated for their cytotoxic activity against HT-29 human colon cancer cells. Compound **1** was found to be the most active in inhibiting the proliferation of HT-29 cancer cells, with an IC₅₀ value of 6.8 μ M. Screening of **1** against CCD-112CoN normal colon cells resulted in an IC₅₀ value of 30.4 μ M. Therefore, the selectivity ratio of compound **1** for cancerous colon cells versus normal colon cells was found to be approximately 4. Microgrewiapipe 3-acetate (**1a**) and compounds **2**, **3**, **5**, and **6** showed IC₅₀ values greater than 10 μ M when evaluated against the HT-29 cancer cell line and were therefore deemed inactive.

Structural similarities between **1–4** and 1-(3-phenylpropyl)-piperidin-3-yl)methyl [1,1'-biphenyl]-2-carboxylate, which was previously identified as a novel ligand of neuronal nicotinic receptors, prompted an examination of the effects of these compounds on nAChRs.¹⁷ In particular, the phenyl rings, the three-carbon aliphatic chain, and the piperidine ring in KAB-18 are comparable to the triene side-chain, aliphatic tail, and piperidinol ring found in **1–4**. The effects of **1–6** and **1a** on human nAChR activity were tested using a functional calcium accumulation assay with HEKtsA201 cells stably expressing either human $\alpha 4\beta 2$ or $\alpha 3\beta 4$ nAChRs. When assayed at a single concentration (10 μ M), all of the natural products (**1–6**) and the semisynthetic acetate analogue (**1a**) inhibited the epibatidine-stimulated calcium accumulation on $\alpha 4\beta 2$ or $\alpha 3\beta 4$ nAChRs (Figure 4, Table 2). This supports their classification as antagonists of human nAChRs. Specifically, compound **1** exhibited approximately 60% and 70% inhibition of $\alpha 4\beta 2$ and $\alpha 3\beta 4$ nAChR activity, respectively. In comparison, the acetate **1a** inhibited approximately 40% of the $\alpha 4\beta 2$ nAChR response (compound **1a** was not tested against $\alpha 3\beta 4$). Analogues incorporating an N-oxide moiety (**2** and **3**) also caused ~80% inhibition for both the $\alpha 4\beta 2$ and $\alpha 3\beta 4$ nAChRs. Microcosamine A (**4**) inhibited 53.7% and 59.0% of the $\alpha 3\beta 4$ and $\alpha 4\beta 2$ activity, respectively. Compounds **5** and **6** produced only weak inhibition of activity for both the $\alpha 3\beta 4$ and $\alpha 4\beta 2$ nAChRs (less than 20% inhibition). The acetate analogue **1a** was synthesized from **1** and shows that compounds with a free hydroxy group at C-3 have more potent activity as nAChR antagonists.

The extent of inhibition shown by these natural products is similar to those of other established nAChR antagonists including bupropion, dihydro- β -erythroidine, *d*-tubocurarine, mecamlamine, tetracaine, and KAB-18-like molecules.^{17,24–26}

Table 2. Percent Inhibition of nAChR Activity by a Single Concentration of Compounds **1–6** and **1a**

compound	$\alpha 3\beta 4$ nAChR	$\alpha 4\beta 2$ nAChR
	% inhibition ^{a,b}	% inhibition ^{a,b}
1	58.2 \pm 9.2	74.0 \pm 14.2
2	82.7 \pm 3.3	79.3 \pm 6.0
3	82.8 \pm 11.5	67.3 \pm 28.0
4	53.0 \pm 9.5	59.0 \pm 7.8
5	14.0 \pm 6.6	21.8 \pm 6.2
6	19.3 \pm 24.4	13.3 \pm 24.5
1a	NT ^c	44.1 \pm 22.3
<i>D</i> -tubocurarine ^d	54.0 \pm 23.5	61.0 \pm 27.9
mecamlamine ^d	88.3 \pm 13.3	91.8 \pm 5.6
KAB-18 ^d	NA ^e	39.0 \pm 11.7

^aPercent inhibition was determined at 10 μ M. ^bValues represent means \pm SD, n = 2–5. ^cNT = not tested. ^dKnown nicotinic receptor antagonist. ^eNA = no activity at 10 μ M.

It is also worth noting the mechanisms by which KAB-18 exerts antagonistic effects on nAChRs. Functional studies with KAB-18 have shown its insurmountable antagonism, suggesting that its activity on nAChRs involves a noncompetitive and allosteric mechanism.¹⁷ That is, KAB-18 does not directly compete with the endogenous ligand acetylcholine for its binding site, but instead acts at a distinct (allosteric) site. Therefore, it has been defined as a negative allosteric modulator of nAChRs. As allosteric modulators can offer significant therapeutic advantages over competitive ligands in clinical practice,¹³ additional attention is warranted on the discovery of natural products, such as compounds **1–4**, which show activity on nAChRs, with a focus on the structural similarities to known allosteric modulators.

Given the evidence implicating nAChRs in the development and progression of cancer, the cytotoxicity of **1–3** against HT-

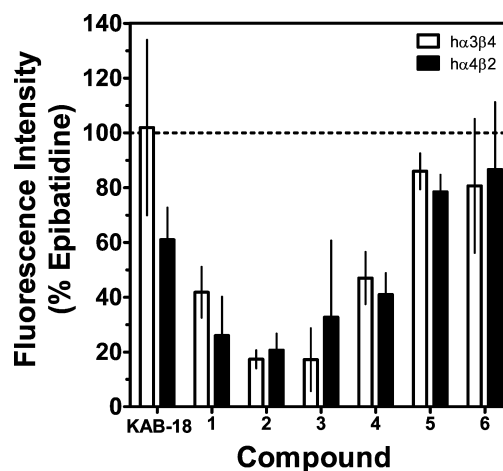


Figure 4. Effects of compounds **1–6** on recombinant nAChRs. An inhibition assay for each compound was performed using HEK tsA201 cells stably expressing $\alpha 3\beta 4$ and $\alpha 4\beta 2$ nAChRs. Cells were loaded with Calcium 5 NW dye and stimulated with 1 μ M epibatidine in the presence of a single concentration of each test compound (10 μ M), as described in the Experimental Section. Results are expressed as the percentage of the control (epibatidine)-stimulated peak fluorescence level. Values represent the means \pm SD of three to five experiments performed in triplicate. Percentage inhibitions achieved by the test compounds are shown in Table 2.

29 human colon cancer cells may be influenced by nAChR modulation. Indeed, there is growing evidence implicating nAChRs in various aspects of cancer development and progression. nAChRs can influence the function, growth, and survival of cancer cells by regulation of a number of neurotransmitters and growth, angiogenic, and neurotrophic factors (e.g., dopamine, glutamate, γ -aminobutyric acid (GABA), serotonin, BDNF, VEGF, HGF, TGF- α , TGF- β , and PDGF).^{18,27} In addition, nAChR activation and the resulting increases in intracellular Ca^{2+} concentrations lead to stimulation of a number of signaling pathways mediating cell proliferation (e.g., Src kinase cascade, PI3-Akt pathway, ERK/MAP kinase cascade, NF- κ B pathway, and cyclic AMP signaling cascade).²⁸ Through activation of antiapoptotic proteins and induction of NF- κ B, nAChRs also directly influence cell survival. Although the *in vitro* cytotoxicity of 1–3 may be influenced by nAChR modulation, exploration of this mechanism is outside the scope of this investigation, but presents a worthy future direction.

Owing to the implication of nAChRs in various diseases and disorders, the discovery of natural compounds with antagonistic activity on nAChRs is of great relevance. In particular, the involvement of nAChRs in various aspects of cancer growth and progression suggests that the cytotoxic effects of compound 1 on HT-29 human colon cancer cells, combined with the nAChR modulation by compounds 1–3, warrant further study. The role of nAChRs in physiological and pathophysiological processes in the central nervous system makes these types of molecules an interesting starting point for drug discovery in this area.

■ EXPERIMENTAL SECTION

General Experimental Procedures. Melting points were determined on a Fisher Scientific melting point apparatus and are uncorrected. Optical rotations were determined on a PerkinElmer 343 automatic polarimeter (sodium lamp). UV spectra were obtained with a PerkinElmer Lambda 10 UV/vis spectrometer. IR spectra were measured on a Thermo Scientific Nicolet 6700 FT-IR spectrometer. NMR spectroscopic data were run on Bruker Avance-300, 400, or 600 MHz spectrometers, and the data were processed using MestReNova 6.0 software. Accurate mass values were obtained on a Micromass LCT ESI spectrometer. Sodium iodide was used for mass calibration for a calibration range of m/z 100–2000. Silica gel (43–60 mesh; Sorbent Technologies, Atlanta, GA, USA) was used for column chromatography. Analytical TLC was performed on precoated 250 μm thickness silica gel plates (UV₂₅₄, glass backed; Sorbent Technologies). HPLC was conducted using a Hitachi LaChrom Elite system composed of a L-2450 diode array detector, a L-2200 autosampler, and a L-2130 pump. Waters X-Bridge C_{18} 5 μm (4.6 \times 150 mm) analytical and 5 μm (10 \times 150 mm) semipreparative HPLC columns were used.

Plant Material. Separate samples of the stem bark, branches and leaves of *Microcos paniculata* were collected in Kego Nature Reserve (18°08.087' N; 105°56.020' E; 40 m alt.), Hatinh Province, Vietnam, in December 2008, by T.N.N., Vuong Tan Tu, and D.D.S., who also identified this plant. A voucher specimen (collection number DDS 14261) has been deposited in the John G. Searle Herbarium of the Field Museum of Natural History, Chicago, Illinois.

Extraction and Isolation. The dried and milled stem bark (646 g), branches (1.1 kg), and leaves (770 g) of *M. paniculata* were extracted separately with methanol. For the stem bark, the MeOH extract (179 g) was concentrated *in vacuo* and partitioned to afford a hexanes extract (2 g) and a CHCl_3 extract (8 g). Bioactivity-guided fractionation of the CHCl_3 -soluble extract (D3) was carried out using an HT-29 human colon cancer cell line and showed an IC_{50} value of 9.9 $\mu\text{g/mL}$. D3 was chromatographed using vacuum-liquid chromatography over silica gel (230–400 mesh) with a step gradient from

hexanes, to EtOAc, to MeOH, producing 11 pooled fractions (F1–F11). Fraction F6 (eluted using EtOAc/10% MeOH) had the most pronounced cytotoxicity (IC_{50} = 6.0 $\mu\text{g/mL}$) and was visualized with Dragendorff's reagent, indicating the presence of alkaloids. Isocratic column chromatographic purification of F6 using silica gel (43–60 mesh; $\text{CHCl}_3/\text{MeOH}$, 15:1) as adsorbent provided 18 further fractions (R1–R18). Fraction R7 was subjected to Sephadex LH-20 column chromatography with elution by 100% MeOH, to afford colorless needles of compound 1 (7 mg).

From the branches of *M. paniculata*, the MeOH extract (39 g) was concentrated *in vacuo* and partitioned to afford a hexanes extract (7 g) and a CHCl_3 extract (6 g). Bioactivity-guided fractionation of the CHCl_3 -soluble extract (D3) was carried out using the HT-29 human colon cancer cell line and showed an IC_{50} value of 13.1 $\mu\text{g/mL}$. D3 was chromatographed over silica gel (230–400 mesh), with a step gradient from hexanes, to EtOAc, to MeOH, producing nine fractions (F1–F9). Fractions F7 and F8 (eluted with EtOAc/10% MeOH) had the most pronounced cytotoxicity, with IC_{50} values of 11.6 and 14.6 $\mu\text{g/mL}$, respectively. The use of Dragendorff's reagent suggested that a group of alkaloids in F7 and F8 could be contributing to the observed cytotoxicity. Purification of F7 employed a reversed-phase (C_{18}) HPLC gradient separation (30:70 $\text{CH}_3\text{CN}/\text{H}_2\text{O}$ to 60:40 $\text{CH}_3\text{CN}/\text{H}_2\text{O}$) over 40 min, affording compound 5 (t_R = 22 min; 3 mg) as the most highly absorbing analyte in the mixture at 205 nm. Passage of F8 over silica gel (43–60 mesh) (eluted with $\text{CHCl}_3/\text{MeOH}$, 15:1) produced 34 fractions, which were combined on the basis of TLC analysis to afford two fractions (R1 and R2). Fraction R1 yielded a yellow, crystalline material, which was purified by reversed-phase HPLC (C_{18}) (5:95 $\text{MeOH}/\text{H}_2\text{O}$ to 95:5 $\text{MeOH}/\text{H}_2\text{O}$) over 60 min, affording compound 6 (t_R = 30 min; 1.3 mg). Fraction R2 was purified by passage over a silica gel (40–63 μm mesh) column ($\text{CHCl}_3/\text{MeOH}$, 10:1 to 5:1), affording four fractions (T1–T4). T2 was purified by reversed-phase HPLC (C_{18}) (48:52 $\text{MeOH}/\text{H}_2\text{O}$ with 0.01% NH_4OH in H_2O mobile phase), to afford microgrewiapipe B (2, t_R = 87 min; 2 mg) as the most highly UV absorbing analyte in the mixture at 270 nm. T3 was purified by reversed-phase HPLC (C_{18}) (30:70 $\text{CH}_3\text{CN}/\text{H}_2\text{O}$ with 0.01% NH_4OH in H_2O mobile phase) to afford microgrewiapipe C (3, t_R = 79 min; 1.5 mg).

From the leaves of *M. paniculata*, the MeOH extract (200 g) was concentrated *in vacuo* and partitioned to afford a hexanes extract (21 g) and a CHCl_3 extract (12 g). Bioactivity-guided fractionation of the CHCl_3 -soluble extract (D3) was carried out using an HT-29 human colon cancer cell line and showed an IC_{50} value of 2.9 $\mu\text{g/mL}$. D3 was chromatographed over silica gel (230–400 mesh), with a step gradient from hexanes, to EtOAc, to MeOH, producing 11 major fractions (F1–F11). F11 (eluted with EtOAc/40% MeOH) had the most pronounced cytotoxicity, with an IC_{50} value of 1.7 $\mu\text{g/mL}$. F11 was loaded onto a Diaion HP-20 column and eluted with 50:50 $\text{MeOH}/\text{H}_2\text{O}$ to obtain a Dragendorff-positive alkaloidal fraction. The retained chlorophyll portion was eluted with pure acetone and stored. F11 was then chromatographed over a silica gel column (43–63 mesh) with a gradient elution ($\text{EtOAc}/\text{CH}_3\text{CN}/\text{H}_2\text{O}/\text{MeOH}$, 70:10:5:5, increasing to 60:20:20:20 of this same solvent mixture), affording four fractions (R1–R4). R1 was further separated by reversed-phase HPLC (C_{18}) (56:44 $\text{CH}_3\text{CN}/\text{H}_2\text{O}$ with 0.01% NH_4OH in H_2O mobile phase), to afford compound 4 (t_R = 46 min; 4.5 mg) along with a minor impurity. Crude 4 was subjected to silica gel (43–63 mesh) chromatography using $\text{CHCl}_3/\text{MeOH}$, 8:1, to afford 4 (0.6 mg) as an amorphous solid.

Microgrewiapipe A (1): colorless needle crystals; mp 127–128 °C; $[\alpha]_D^{25} +15.4$ (c 1.0, MeOH); UV (MeOH) λ_{max} (log ϵ) 270 (3.87) nm; IR (film) ν_{max} 3402, 2956, 2923, 2864 cm^{-1} ; ^1H NMR (600 MHz, CDCl_3) and ^{13}C NMR (150 MHz, CDCl_3) data, see Table 1; HRESIMS m/z 264.2329 $[\text{M} + \text{H}]^+$ (calcd for $\text{C}_{17}\text{H}_{30}\text{NO}$, 264.2327).

Preparation of Microgrewiapipe A 3-Acetate (1a). A catalytic amount of *N,N*-dimethylaminopyridine (0.1 equiv) and 5 mg of 1 were placed in a round-bottomed flask under argon. Anhydrous dichloromethane (500 μL) was added, and the mixture was cooled to 0 °C. Triethylamine (2 equiv) was added, followed by dropwise addition of acetic anhydride (3 equiv), and the reaction was warmed to room temperature and stirred for 3 h. The reaction was quenched with a

saturated aqueous NaHCO_3 solution at 0 °C. The mixture was extracted two times with ethyl acetate (50 mL), and the combined organic layers were washed with brine, dried over Na_2SO_4 , filtered, and evaporated in vacuo. The crude product was chromatographed over silica gel ($\text{CHCl}_3/\text{MeOH}/\text{AcOH}$, 10:1:0.1) to yield **1a** as a white, amorphous solid (3 mg, 60%).

Microgrewiapipe A 3-acetate (1a): amorphous solid; $[\alpha]_D^{25} +19.5$ (c 1.0, MeOH); UV (MeOH) λ_{max} (log ϵ) 259 (4.29) nm; ^1H NMR (400 MHz, CDCl_3) δ_{H} 0.87 (3H, t, $J = 7.0$ Hz, H-10'), 1.11 (3H, d, $J = 5.8$, CH_3 -2 α), 1.30 (1H, m, H-2 β), 1.31–1.42 (1H, m, H-4 α), 1.31–1.42 (2H, m, H-8', 9'), 1.35 (1H, m, H-5 α), 1.55 (1H, ddd, $J = 13.2$, 3.3, 2.0 Hz, H-5 β), 1.69 (1H, m, H-4 β), 2.05 (3H, s, OCOCH_3), 2.12 (1H, m, H-7'), 2.21 (3H, s, N- CH_3), 2.54 (1H, ddd, $J = 11.2$, 8.6, 3.4 Hz, H-6 β), 4.48 (1H, ddd, $J = 10.6$, 7.3, 2.6 Hz, H-3 α), 5.55 (1H, dt, $J = 14.4$, 8.8, H-1'), 5.72 (1H, dd, $J = 7.1$, 7.0, H-6'), 6.04–6.18 (4H, m, H-2'-5'), ^{13}C NMR (100 MHz, CDCl_3) δ_{C} 170.7 (OCOCH_3), 137.4 (C-1'), 136.7 (C-6'), 130.8–133.6 (C-2'-C-5'), 75.1 (C-3), 67.2 (C-6), 33.7 (C-7'), 32.3 (C-4), 31.4 (C-8'), 30.3 (C-5), 22.4 (C-9'), 21.8 (C-2), 14.7 (C-10'); HRESIMS m/z 306.2419 $[\text{M} + \text{H}]^+$ (calcd for $\text{C}_{19}\text{H}_{31}\text{NO}_2$, 306.2433).

Preparation of MTPA Esters of Microgrewiapipe A (1). A modified Mosher ester procedure carried out directly in NMR tubes was used as previously reported.^{21,22} After drying compound **1** (2 mg, 0.0078 mmol) in the NMR tube overnight in a desiccator, approximately 400 μL of pyridine- d_5 were added under argon. Separate 2 mg portions of **1** were treated with (S)- α -methoxy- α -(trifluoromethyl)phenylacetyl chloride and (R)-MTPA-Cl (0.075 mmol, 10 equiv) at room temperature. After 6 h, the reaction was complete and the ^1H NMR (400 MHz, CDCl_3) and ^1H – ^1H COSY spectra were recorded. Ambiguous and overlapping signals were not used for the $\Delta\delta_{\text{S-R}}$ calculations.^{21,22} ^1H NMR data of (R)-MTPA ester of **1** (400 MHz, pyridine- d_5): δ 2.60 (3H, s, N- CH_3), 2.37 (1H, m, H-5), 1.89 (1H, m, H-4 α), 1.50 (2H, m, H-4 β), 1.25 (3H, m, CH_3 -2). ^1H NMR data of (S)-MTPA ester of **1** (400 MHz, pyridine- d_5): δ 2.56 (3H, s, N- CH_3), 2.42 (1H, m, H-5), 1.91 (1H, m, H-4 α), 1.64 (2H, m, H-4 β), 1.12 (3H, m, CH_3 -2).

Microgrewiapipe B (2): amorphous solid; mp 134–136 °C; $[\alpha]_D^{25} +4.0$ (c 0.1, MeOH); UV (MeOH) λ_{max} (log ϵ) 272 (3.97) nm; IR (film) ν_{max} 3400, 2967, 1670, 1204, 1000 cm^{-1} ; ^1H NMR (400 MHz, CDCl_3) and ^{13}C NMR (100 MHz, CDCl_3) data, see Table 1; HRESIMS m/z 280.2269 $[\text{M} + \text{H}]^+$ (calcd for $\text{C}_{17}\text{H}_{30}\text{NO}_2$, 280.2276).

Microgrewiapipe C (3): colorless needle crystals; mp 130–131 °C; $[\alpha]_D^{25} +77.8$ (c 0.1, MeOH); UV (MeOH) λ_{max} (log ϵ) 274 (3.92) nm; IR (film) ν_{max} 3400, 2967, 1670, 1204, 1000 cm^{-1} ; ^1H NMR (400 MHz, CDCl_3) and ^{13}C NMR (100 MHz, CDCl_3) data, see Table 1; HRESIMS m/z 280.2281 $[\text{M} + \text{H}]^+$ (calcd for $\text{C}_{17}\text{H}_{30}\text{NO}_2$, 280.2277).

Cytotoxicity Assays. Isolation was directed using a gatekeeper assay that tests cytotoxicity toward HT-29 human colon cancer cells. Compounds **1**–**6** were evaluated in this assay and showed a range of activities according to a previously described protocol.¹⁴ Paclitaxel was used as a positive control and exhibited an IC_{50} value of 0.001 μM .

Compound **1** and paclitaxel were screened also against a normal colon cell line (CCD-112CoN). Compounds with an IC_{50} value less than 10 μM against HT-29 cells were further tested against the CCD-112CoN normal colon cell line. For this assay, CCD-112CoN noncancerous human colon cells (ATCC, CRL-1541) were cultured in MEME medium (Hyclone, Logan, UT, USA) supplemented with 10% FBS, PSF, 1.0 mM sodium pyruvate, 0.1 mM nonessential amino acid, and 1.5 g/L sodium bicarbonate and placed in a humidified incubator with an atmosphere of 95% air and 5% CO_2 at 37 °C. Cells were trypsinized and split for subculture when they reached near-confluent state (5 days or later). Upon reaching about 70% confluence, the medium was changed and the cells were used for the test procedure one day later. The harvested cells, after appropriate dilution, were seeded per well in 96-well CCD-112CoN normal colon cells (7600 cells/190 μL) plates using complete medium and were treated with the test samples (10 μL /well in triplicate) at various concentrations. Test samples were performed using 10% DMSO as the solvent. Then, 10 μL of 10% DMSO was also added to the control wells. After incubation for 3 days at 37 °C in 5% CO_2 , the cells were fixed to the

plates by the addition of 100 μL of cold 20% trichloroacetic acid and incubated at 4 °C for 30 min. Next, the plates were washed three times with tap water and dried overnight. The fixed cells were stained for 30 min at room temperature with 0.4% (w/v) sulforhodamine B, an anionic protein stain in 1% acetic acid, and rinsed three times with 1% acetic acid to remove unbound dye and allowed to dry. The bound dye was then solubilized with 10 mM unbuffered Tris base (pH 10, 200 μL /well) for 5 min on a shaker. Absorbance at 515 nm was measured with a Bio-Tek μQuant microplate reader. The IC_{50} values of test samples in serial dilutions were calculated using nonlinear regression analysis (TableCurve 2D v4; AISN Software, Inc., Mapleton OR, USA). Paclitaxel exhibited an IC_{50} value of 23.0 μM against CCD-112CoN normal colon cells.

Calcium Accumulation Assays. Calcium accumulation assays were performed with HEK ts201 cells stably expressing either human $\alpha 3\beta 4$ nAChRs ($\text{h}\alpha 3\beta 4$ nAChRs) or human $\alpha 4\beta 2$ nAChRs ($\text{h}\alpha 4\beta 2$ nAChRs) (obtained from Professor Jon Lindstrom, University of Pennsylvania, Philadelphia, PA, USA), using a previously reported procedure.^{17,24,26} Cells were plated at a density of 2.0 to 2.3×10^5 cells per well in poly-L-ornithine-coated 96-well culture plates 24 h prior to the assay. On the day of experiments, cells were washed with 100 μL of HEPES-buffered Krebs (HBK) and incubated with 40 μL of HBK and 40 μL of Calcium 5 NW dye (Molecular Devices, Sunnyvale, CA, USA) (1 h, room temperature). Changes in intracellular calcium levels resulting from nAChR activation were then measured simultaneously during and after the course of drug treatment period using a fluid handling integrated fluorescence plate reader (FlexStationII, Molecular Devices, Sunnyvale, CA, USA). In order to evaluate the antagonistic effects of compounds, cells were treated with the compounds at the first addition (20 s) and with 1 μM of the nAChR agonist epibatidine (Thermo Fisher Scientific, Pittsburgh, PA, USA) at the second addition (60 s) in the continued presence of the compounds. For the quantification of compound antagonistic effects, a control-agonist-treated group and a control-sham group were included. For the control-agonist group, HBK (40 μL) and 1 μM epibatidine solution (40 μL) were added at the first and second treatment period, respectively. The control-sham group was treated with HBK (40 μL) at the first and second treatment period, respectively. The changes in fluorescence were measured continuously for 120 s from the bottom of the well at an excitation of 485 nm and emission of 525 nm at ca. 1.5 s intervals. Functional responses were quantified by first calculating the net fluorescence (the difference between control-agonist-treated group and control-sham group), and results were expressed as a percentage of control-agonist group (1 μM epibatidine). All functional data were calculated from the number of observations performed in triplicate. For pharmacological evaluation, compounds were initially prepared with 100% DMSO (0.01 M stocks). Further dilutions of compounds were made in HBK buffer (≤ 100 μM).

■ ASSOCIATED CONTENT

● Supporting Information

NMR spectroscopic data for compounds **1**–**3** including ^1H , ^{13}C , and 2D NMR spectra and ESIMS/MS data of the new compounds **1**–**3**. This material is available free of charge via the Internet at <http://pubs.acs.org>.

■ AUTHOR INFORMATION

Corresponding Author

*Tel: +1-614-247-8094. Fax: +1-614-247-8081. E-mail: kinghorn.4@osu.edu.

Notes

The authors declare no competing financial interest.

■ ACKNOWLEDGMENTS

This study was supported, in part, by grant P01 CA125066 (awarded to A.D.K.) from NCI, NIH. *Microcos paniculata* samples were collected under the terms of an agreement

between the University of Illinois at Chicago and the Institute of Ecology and Biological Resources (IEBR) of the Vietnam Academy of Science and Technology, Hanoi, Vietnam. We thank the Director of Kego Nature Reserve for the permission, and Dr. L. X. Canh, Director of IEBR, for the support and facilitation in the collection of the plant material. Prof. J. Lindstrom, University of Pennsylvania, Philadelphia, PA, provided HEK tsA201 cells stably expressing either $\alpha 4\beta 2$ or $\alpha 3\beta 4$ nAChRs. We acknowledge Mr. J. Fowble, College of Pharmacy, The Ohio State University, and Dr. C.-H. Yuan, OSU Campus Chemical Instrument Center, for facilitating the acquisition of the 400 and 600 MHz NMR spectra. We acknowledge Ms. N. Kleinholz, Mr. M. Apsaga, and Dr. K. Green-Church, Campus Chemical Instrument Center, The Ohio State University, for the mass spectrometric measurements. We acknowledge Dr. P. N. Patil, Professor Emeritus, College of Pharmacy, The Ohio State University, for facilitating this collaborative investigation and for many helpful suggestions.

■ REFERENCES

- (1) Dorr, L. J. In *Flora of China*, Vol. 12; Wu, Z. Y.; Raven, P. H.; Hong, D. Y., Eds.; Science Press, Beijing, and Missouri Botanical Garden Press: St. Louis, MO, 2007; pp 251–258, 1753.
- (2) Luo, J. *Acta Pharm. Sin.* **2009**, *44*, 150–153.
- (3) Bandara, K. A. N. *Phytochemistry* **2000**, *54*, 29–32.
- (4) Feng, S.-X.; Lin, L.-D.; Xu, H.-H.; Wei, X.-Y. *J. Asian Nat. Prod. Res.* **2008**, *10*, 1155–1158.
- (5) Linquist, N.; Shigematsu, N.; Pannell, L. J. *Nat. Prod.* **2000**, *63*, 1290–1291.
- (6) MacConnell, J. G.; Blum, M. S. *Science* **1970**, *168*, 840–841.
- (7) Yi, G. B.; McClendon, D.; Desai, D.; Goddard, J.; Lister, A.; Moffitt, J.; Vander Meer, R. K.; deShazo, R.; Lee, K. S.; Rockhold, R. W. *Int. J. Toxicol.* **2003**, *22*, 81–86.
- (8) Chen, L.; Sharma, K. R.; Fadamiro, H. Y. *Naturwissenschaften* **2009**, *96*, 1421–1429.
- (9) Gotti, C.; Riganti, L.; Vailati, S.; Lementi, F. *Curr. Pharm. Des.* **2006**, *12*, 407–428.
- (10) Lukas, R. J.; Changeux, J.-P.; Le Novère, N.; Albuquerque, E. X.; Balfour, D. J. K.; Berg, D. K.; Bertrand, D.; Chiappinelli, V. A.; Clarke, P. B. S.; Collins, A. C.; Dani, J. A.; Grady, S. R.; Kellar, K. J.; Lindstrom, J. M.; Marks, M. J.; Quik, M.; Taylor, P. W.; Wonnacott, S. *Pharmacol. Rev.* **1999**, *51*, 397–401.
- (11) Gotti, C.; Riganti, L.; Vailati, S.; Lementi, F. *Curr. Pharm. Des.* **2006**, *12*, 407–428.
- (12) Dani, J. A.; Bertrand, D. *Annu. Rev. Pharmacol. Toxicol.* **2007**, *47*, 699–729.
- (13) Taly, A.; Corringier, P.-J.; Guedin, D.; Lestage, P.; Changeux, J.-P. *Nat. Rev. Drug Discovery* **2009**, *8*, 733–750.
- (14) Pan, L.; Kardono, L. B. S.; Riswan, S.; Chai, H.; Carcache de Blanco, E. J.; Pannell, C. M.; Soejarto, D. D.; McCloud, T. G.; Newman, D. J.; Kinghorn, A. D. *J. Nat. Prod.* **2010**, *73*, 1873–1878.
- (15) Anis, E.; Anis, I.; Ahmed, S.; Mustafa, G.; Malik, A.; Afza, N.; Hai, S. M. A.; Shahzad-ul-Hussan, S.; Choudhary, M. I. *Chem. Pharm. Bull.* **2002**, *50*, 112–114.
- (16) Harrigan, G. G.; Gunatilaka, A. A. L.; Kingston, D. G. I. *J. Nat. Prod.* **1994**, *57*, 68–73.
- (17) Henderson, B. J.; Pavlovicz, R. E.; Allen, J. D.; González-Cestari, T. F.; Orac, C. M.; Bonnell, A. B.; Zhu, M. X.; Boyd, R. T.; Li, C.; Bergmeier, S. C.; McKay, D. B. *J. Pharmacol. Exp. Ther.* **2010**, *334*, 761–774.
- (18) Schuller, H. M. *Nat. Rev. Cancer* **2009**, *9*, 195–205.
- (19) Egleton, R. D.; Brown, K. C.; Dasgupta, P. *Trends Pharmacol. Sci.* **2008**, *29*, 151–158.
- (20) Ando, T.; Ogura, Y.; Koyama, M.; Kurane, M.; Uchiyama, M.; Seol, K. Y. *Agric. Biol. Chem.* **1988**, *52*, 2459–2468.
- (21) Reiser, M. J.; Hui, Y. H.; Rupprecht, J. K.; Kozlowski, J. F.; Wood, K. V.; McLaughlin, J. L.; Hanson, P. R.; Zhuang, Z.; Hoye, T. R. *J. Am. Chem. Soc.* **1992**, *114*, 10203–10213.
- (22) Su, B.-N.; Park, E. J.; Mbawambo, Z. H.; Santarsiero, B. D.; Mesecar, A. D.; Fong, H. H. S.; Pezzuto, J. M.; Kinghorn, A. D. *J. Nat. Prod.* **2002**, *65*, 1278–1282.
- (23) Frisch, M. J.; Trucks, G. W.; Schlegel, H. B.; Scuseria, G. E.; Robb, M. A.; Cheeseman, J. R.; Scalmani, G.; Barone, V.; Mennucci, B.; Petersson, G. A.; Nakatsuji, H.; Caricato, M.; Li, X.; Hratchian, H. P.; Izmaylov, A. F.; Bloino, J.; Zheng, G.; Sonnenberg, J. L.; Hada, M.; Ehara, M.; Toyota, K.; Fukuda, R.; Hasegawa, J.; Ishida, M.; Nakajima, T.; Honda, Y.; Kitao, O.; Nakai, H.; Vreven, T.; Montgomery, J. A., Jr.; Peralta, J. E.; Ogliaro, F.; Bearpark, M.; Heyd, J. J.; Brothers, E.; Kudin, K. N.; Staroverov, V. N.; Kobayashi, R.; Normand, J.; Raghavachari, K.; Rendell, A.; Burant, J. C.; Iyengar, S. S.; Tomasi, J.; Cossi, M.; Rega, N.; Millam, J. M.; Klene, M.; Knox, J. E.; Cross, J. B.; Bakken, V.; Adamo, C.; Jaramillo, J.; Gomperts, R.; Stratmann, R. E.; Yazyev, O.; Austin, A. J.; Cammi, R.; Pomelli, C.; Ochterski, J. W.; Martin, R. L.; Morokuma, K.; Zakrzewski, V. G.; Voth, G. A.; Salvador, P.; Dannenberg, J. J.; Dapprich, S.; Daniels, A. D.; Farkas, Ö.; Foresman, J. B.; Ortiz, J. V.; Cioslowski, J.; Fox, D. J. *Gaussian 09*, Revision A.01; Gaussian, Inc.: Wallingford, CT, 2009.
- (24) González-Cestari, T. F.; Henderson, B. J.; Pavlovicz, R. E.; McKay, S. B.; El-Hajj, R. A.; Pulipaka, A. B.; Orac, C. M.; Reed, D. D.; Boyd, R. T.; Zhu, M. X.; Li, C.; Bergmeier, S. C.; McKay, D. B. *J. Pharmacol. Exp. Ther.* **2009**, *328*, 504–515.
- (25) McKay, D. B.; Chang, C.; González-Cestari, T. F.; McKay, S. B.; El-Hajj, R.; Bryant, D. L.; Zhu, M. X.; Swann, P. W.; Arason, K. M.; Pulipaka, A. B.; Orac, C. M.; Bergmeier, S. C. *Mol. Pharmacol.* **2007**, *71*, 1288–1297.
- (26) Henderson, B. J.; Carper, D. J.; González-Cestari, T. F.; Yi, B.; Dalefield, M. L.; Coleman, R. S.; McKay, D. B. *J. Med. Chem.* **2011**, *54*, 8681–8692.
- (27) Paleari, L.; Grozio, A.; Cesario, A.; Russo, P. *Sem. Cancer Biol.* **2008**, *18*, 211–217.
- (28) Dasgupta, P.; Kinkade, R.; Joshi, B.; Decook, C.; Haura, E.; Chellappan, S. *Proc. Natl. Acad. Sci.* **2006**, *103*, 6332–6337.